Theoretical modeling of the OH stretch infrared spectrum of carboxylic acid dimers based on first-principles anharmonic couplings

Gina M. Florio and Timothy S. Zwier
Department of Chemistry, Purdue University, West Lafayette, Indiana 47907-1393

Evgeniy M. Myshakin and Kenneth D. Jordan[a)]
Department of Chemistry and Center for Molecular and Materials Simulations, University of Pittsburgh, Pittsburgh, Pennsylvania 15260

Edwin L. Sibert III[b)]
Theoretical Chemistry Institute, Department of Chemistry, University of Wisconsin, Madison, Wisconsin 53706-1396

(Received 20 September 2002; accepted 28 October 2002)

Carboxylic acid dimers serve as prototypical systems for modeling the unusual spectral behavior of the hydride stretch fundamental. Large anharmonic effects associated with the pair of cooperatively strengthened OH···O═C hydrogen bonds produces complicated infrared spectra in which the OH stretch oscillator strength is spread over hundreds of wave numbers, resulting in a complicated band sub-structure. In this work cubic anharmonic constants are computed along internal coordinates associated with the intramolecular OH stretch, intermolecular stretch, and OH bend internal coordinates for the formic acid and benzoic acid dimers. These are then projected onto the normal coordinates to produce mixed states that are used in computing the OH stretch infrared spectrum. For the benzoic acid dimer the calculations accurately reproduce for three deuterated isotopomers the overall breadth and much of the vibrational sub-structure in the observed spectra. For the formic acid dimer, the spectrum is calculated using a model employing a subset of the cubic force constants as well as using the full cubic force field. The spectra calculated for the formic acid dimer are sparser and somewhat more sensitive to the exact positions of the anharmonically coupled states than that of the benzoic acid dimer. Again semiquantitative agreement with experiment is obtained.
 [DOI: 10.1063/1.1530573]

I. INTRODUCTION

The hydride stretch region of infrared spectra has long been used to diagnose the presence and strength of hydrogen bonds involving the XH group.[1] When an XH group forms a hydrogen bond, the XH stretch fundamental undergoes a large frequency shift, the magnitude of which reflects the strength of the hydrogen bond formed. Accompanying this frequency shift is a corresponding broadening and increase in the infrared intensity of the XH fundamental. The infrared (IR) spectra of the carboxylic acid dimers manifest all of these effects. These species are particularly interesting because they are held together by two cooperatively strengthened OH···O═C hydrogen bonds. In symmetric carboxylic acid dimers, such as the formic acid,[2–4] acetic acid,[5] or benzoic acid[6] homodimers shown below, the OH stretch bands are spread over more than 500 cm^{-1}, and exhibit a rich substructure that reflects the presence of strong anharmonic couplings.

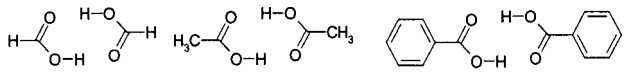

Formic acid dimer Acetic acid dimer Benzoic acid dimer

Much past theoretical work on these species has sought to determine the most important sources of the broadening and sub-structure in the OH stretch region of the spectra. Here, we return to these issues, motivated by new infrared spectra obtained under supersonic jet conditions of the formic acid dimer,[2,3] the acetic acid dimer,[5] and three isotopomers of the benzoic acid dimer.[6] The cooling under these conditions collapses the population entirely into the zero-point vibrational level (which can be split by tunneling). Furthermore, in the case of the benzoic acid dimer, the double resonance scheme employed (fluorescence-dip infrared spectroscopy) ensures that the observed spectral absorptions are uncontaminated by hot bands, but instead arise purely from the zero-point level, with a rotational distribution in the 3–5 Kelvin temperature range.[6] Such conditions resolve substructure that would be obscured in the presence of hot bands. Furthermore, the selectivity of the double resonance scheme also enables the acquisition of infrared spectra from individual deuterated isotopomers free from interference from one another.

In a recent paper we presented initial results of a theoretical model which sought to account quantitatively for the structure observed in the OH stretch spectrum of the benzoic acid dimer.[6] This model was able to account for the overall breadth of the spectrum as well as for the major sub-structure observed. The present paper provides a full account of the model, building on the initial results in several ways.

[a)]Author to whom correspondence should be addressed. Electronic mail: jordan@imap.pitt.edu
[b)]Author to whom correspondence should be addressed. Electronic mail: elsibert@facstaff.wisc.edu

In Sec. II the relationship of the current work to prior theoretical approaches to the vibrational spectra of H-bonded dimers is briefly reviewed. Section III develops the theoretical model used in this work. Section IV provides computational results that serve as input for the theory. These involve an extensive set of electronic structure calculations of the geometries, harmonic vibrational frequencies, and key anharmonic constants for the formic acid dimer (FAD) and for the benzoic acid dimer (BAD). The ability of the simple physical model, employing only a subset of the anharmonic couplings, to capture the important physics is established by carrying out for FAD a calculation of the spectrum using the full cubic force field. Finally, in Sec. V, the model is applied to formic acid dimer and three isotopomers of benzoic acid dimer. We shall see that much of the sub-structure in the IR spectra of these dimers can be accounted for by a single cubic anharmonic term coupling the OH stretch and OH bend internal coordinates.

II. BACKGROUND MATERIAL

The goal of the present study is to generate vibrational spectra of FAD and BAD in the region of the OH fundamental, allowing for cubic couplings. There is a considerable body of previous theoretical work in this area starting with the early studies of Bratos and Hadzi[7] and Sheppard.[8] For a recent review, the reader is referred to the work of Chamma and Henri-Rousseau.[9] In cyclic H-bonded dimers the main couplings appear to be Davydov coupling between the two localized OH stretch vibrations, Fermi coupling between the OH stretch and nearly resonant combination bands, and coupling between OH stretch and interdimer H-bond vibrations.

Maréchal and Witkowski[10] have modeled the complex structure of the acetic acid dimer using an adiabatic treatment that describes the coupling of the high frequency X···H and low frequency X···Y vibrations. This model, using empirically determined coupling constants, provided good agreement with experiment. Wócjik *et al.*[11] used instead *ab initio* methods to calculate the relevant cubic potential couplings, and concluded that the coupling between the OH stretch and intermolecular H-bond vibrations does not account for the observed spectrum. However, because the calculations were at the Hartree–Fock level and employed the small 4-31G basis set, the results should be considered qualitative at best.

Subsequently Maréchal reanalyzed the IR spectra of carboxylic acid dimers in the gas phase,[12] highlighting the role of the so-called ''parasitic'' Fermi resonances. From his perspective, Fermi resonances complicate the analysis of the IR spectra, hiding the more interesting, temperature-dependent effects of the coupling of the OH stretch with the lower frequency modes. Using an elegant deconvolution procedure,[13] Maréchal removed the effects of the Fermi resonances, obtaining spectra, with relatively narrow full width at half maximum (FWHM), and which, in principle, include effects due to coupling with the low frequency modes only. To the best of our knowledge, there has been no attempt to verify these results by comparing with spectra calculated using *ab initio* values of the coupling constants.

Very recently, Ito and Nakanaga[2,3] have obtained high-resolution jet-cooled infrared spectra of FAD by cavity ring down spectroscopy. These low temperature spectra are much less congested than the earlier room temperature spectra, as expected if coupling to low-frequency modes were the dominant contributors to the width of the spectra in the latter and supporting the conclusions of Maréchal.[12]

III. THEORETICAL MODEL

This section describes the calculation of potential couplings and the theoretical models used to calculate the vibrational spectra of BAD and FAD. For BAD only a limited set of potential couplings are calculated, with the choice of couplings being motivated by the prior studies described above. In particular, we incorporate the cubic force constants that couple the OH stretch to the OH bending and to the intermolecular H-bond stretching degrees of freedom. In order to test the appropriateness of this truncated cubic force field approach, it was also applied to FAD, for which spectra are also calculated using the full cubic force field.

We first describe the truncated force field model, as applied to BAD. However, other than the labeling of the coordinates, and the need to account also for the CH stretch vibrations, the model is also applicable to FAD. The calculation of the IR spectra proceeds *via* a three-stage process. We first choose local internal coordinates that are linear combinations of the normal coordinates. Although there is no fundamental reason for the internal coordinates to be linearly related to the normal coordinates, this choice simplifies the transformation between the two coordinate systems. We then obtain using electronic structure methods a restricted cubic force field as a function of the internal coordinates. The resulting force field is then re-expanded as a function of the normal coordinates. The vibrational spectrum is obtained by diagonalizing the resulting Hamiltonian in a basis set that consists of states that are directly coupled to the OH fundamental, and, as such, the resulting spectrum includes all possible coupling mechanisms considered in earlier research. The remainder of this section describes these steps in more detail.

A. Choice of coordinates

The standard approach for determining the relation between internal coordinates, **R**, and Cartesian coordinates, **x**, is to construct the **B**-matrix of Wilson, Decius, and Cross[14]

$$\mathbf{R}=\mathbf{B}\mathbf{x}. \tag{1}$$

The Cartesian coordinates, in turn, are linearly related to the normal coordinates **Q** via the ℓ-matrix as

$$\mathbf{x}=\ell\mathbf{Q}, \tag{2}$$

which itself is the output of a normal mode calculation. Combining Eqs. (1) and (2), we obtain the transformation between internal and normal coordinates

$$\mathbf{R}=\mathbf{B}\ell\mathbf{Q}=\mathbf{L}\mathbf{Q}. \tag{3}$$

For the set of **R** coordinates to be linearly related to the normal coordinates, the elements of the **B**-matrix must be

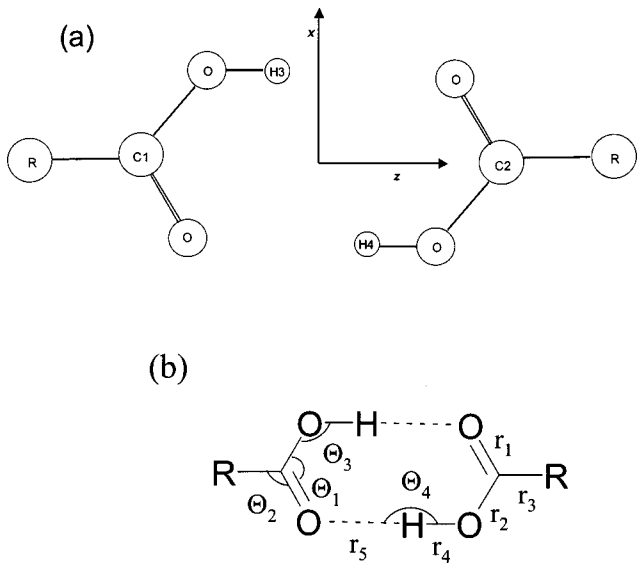

FIG. 1. (a) Schematic diagram showing the labeling of the position of the atoms; (b) Geometrical parameters in the formic and benzoic acid dimers. Here R═H, Ph.

constants. This is achieved by defining the internal symmetry coordinates in terms of the Cartesian extension coordinates depicted in Fig. 1:

$$\begin{aligned} R_1 &= z_2 - z_1, \\ R_2 &= (z_3 - z_4) - (z_1 - z_2), \\ R_3 &= (z_3 + z_4) - (z_1 + z_2), \\ R_4 &= (x_3 - x_4) - (x_1 - x_2), \\ R_5 &= (x_3 + x_4) - (x_1 + x_2). \end{aligned} \tag{4}$$

The overall molecule is oriented so that the OH bonds are parallel to the z axis. With these definitions, R_1 corresponds to the interdimer stretch, R_2 and R_3 correspond to the symmetric and antisymmetric OH stretch coordinates, respectively, and R_4 and R_5 correspond to the symmetric and antisymmetric OH bend coordinates, respectively. In defining these coordinates it has been assumed that the RCO_2 entities are rigid. As such, the centers-of-mass of the monomers rather than the carbon atoms could have been selected to describe their relative motion. The remaining vibrational coordinates are assumed to correspond to atomic motions with respect to the center of masses of the monomers and rotations of the monomers.

The elements of the **B**-matrix can be readily extracted from Eq. (4). Since the normal-mode calculation provides the ℓ-matrix, Eq. (3) completes the transformation between internal and normal coordinates. In this work, the cubic force constants are calculated in terms of the internal coordinates using finite difference methods. To accomplish this, it is useful to construct the inverse of the **B**-matrix, which is done by introducing the appropriate constraints, i.e., the center-of-mass and Eckart conditions. The details of these transformations are described in the Appendix.

B. Choice of cubic coupling terms

In the truncated cubic force field, the key coupling terms involving the OH stretch fundamentals are divided into two contributions:

$$V = V_{sb} + V_{ss}, \tag{5}$$

where V_{sb} is the OH stretch–bend force field which takes the form

$$V_{sb} = f_{345} R_3 R_4 R_5 + \frac{1}{2} f_{244} R_2 R_4 R_4 + \frac{1}{2} f_{255} R_2 R_5 R_5, \tag{6}$$

and V_{ss} is the OH stretch-H-bond stretch force field which is of the form

$$V_{ss} = \frac{1}{2} f_{122} R_1 R_2 R_2 + \frac{1}{2} f_{133} R_1 R_3 R_3. \tag{7}$$

C. Calculation of spectra

To calculate the spectra, the potential given by Eqs. (5)–(7) is re-expressed in terms of the normal coordinates using Eq. (4). This yields the cubic force field

$$V(Q) = \frac{1}{6} \sum_i \sum_j \sum_k F_{i,j,k} Q_i Q_j Q_k. \tag{8}$$

This is tantamount to projecting the potential couplings involving the OH stretch modes onto the normal coordinates of the molecule. The largest contributions to the potential of Eq. (8) can be separated into stretch–stretch and stretch–bend components as in Eq. (5). For $h6$-$h6$ BAD this is straightforward, since the antisymmetric OH stretch character and the interdimer stretch character are both contained primarily in one normal coordinate (Q_{12} and Q_{77}, respectively). (The numbering scheme for the normal modes of BAD is defined in Table III, below.) The coupling terms involving the symmetric OH stretch normal coordinate have been omitted since this mode is infrared inactive, but these terms are necessary when considering the partially deuterated BAD isotopomers. With this in mind, Eq. (8) reduces in the case of BAD to

$$V(Q) \cong \tfrac{1}{2} \sum_i \sum_j F_{i,j,12} Q_i Q_j Q_{12} + \tfrac{1}{2} F_{77,12,12} Q_{77} Q_{12} Q_{12}. \tag{9}$$

The first term includes the stretch–bend coupling that leads to Fermi resonances, and the second term corresponds the stretch–stretch coupling that leads to progressions in the interdimer mode. It is important to note that the term involving the sum over i and j also includes coupling to normal modes other than the COH bends. This is a consequence of the bend local modes having sizable projections onto several normal modes.

The cubic force field is combined with the standard normal-mode Hamiltonian, and the spectrum calculated by diagonalizing the resulting Hamiltonian matrix in a basis set that includes the ground state, the IR active OH stretch fundamental, all combination states that are directly (Fermi) coupled to this fundamental and that have energies within 600 cm^{-1} of the fundamental. In addition, the basis includes progressions built on these vibrational states (including the zero-point level) involving the low-frequency interdimer nor-

TABLE I. The key geometrical parameters [cf. Fig. 1(b)] of the formic and benzoic acid monomer and dimers.

		Formic acid								Benzoic acid	
		B3LYP				MP2				B3LYP	
	Expt[a]	6-31+G(d)	6-311+G ($2d,p$)	aug-cc-pVDZ	aug-cc-pVTZ	6-311+G ($2d,p$)	aug-cc-pVDZ	aug-cc-pVTZ	Expt[b]	6-31G (d,p)	Mixed[c]
					Monomer						
r_1 (A)	1.202±0.003	1.207	1.198	1.205	1.198	1.205	1.215	1.205	···	1.215	1.208
r_2 (A)	1.343±0.003	1.348	1.345	1.349	1.345	1.340	1.359	1.347	···	1.358	1.358
r_3 (A)	1.097±0.021	1.098	1.097	1.103	1.096	1.090	1.103	1.097	···	1.486	1.485
r_4 (A)	0.972±0.017	0.978	0.972	0.973	0.971	0.970	0.975	0.971	···	0.972	0.967
Θ_1(deg)	124.6±0.5	125.1	125.1	125.0	125.1	125.1	125.1	125.0	···	121.9	121.7
Θ_2(deg)	124.1±3.1	125.3	125.2	125.1	125.1	125.2	125.3	125.3	···	125.0	125.0
Θ_3(deg)	106.3±0.4	107.8	107.6	107.5	107.8	106.7	106.3	106.4	···	105.6	106.3
					Dimer						
r_1 (A)	1.217±0.003	1.225	1.219	1.226	1.218	1.224	1.233	1.224	1.263	1.237	1.229
r_2 (A)	1.320±0.003	1.318	1.310	1.315	1.310	1.316	1.325	1.313	1.275	1.320	1.321
r_3 (A)	1.079±0.021	1.097	1.096	1.102	1.095	1.094	1.101	1.096	1.484	1.487	1.485
r_4 (A)	1.033±0.017	1.003	1.004	1.006	1.002	1.001	1.001	1.000	···	1.009	1.001
r_5 (A)	-	1.720	1.662	1.659	1.667	1.671	1.684	1.654	···	1.608	1.647
Θ_1(deg)	126.2±0.5	126.3	126.3	126.3	126.3	126.3	126.4	126.3	123.2	123.7	123.3
Θ_2(deg)	115.4±3.1	122.1	121.8	121.7	121.8	121.9	122.1	121.9	120.2	121.7	122.1
Θ_3(deg)	108.5±0.4	110.6	110.7	110.6	110.9	109.7	109.2	109.5	···	110.4	110.3
Θ_4(deg)	180[d]	176.9	178.7	179.1	178.5	179.4	179.7	180.0	···	179.0	181.4

[a]References 19 and 20.
[b]The experimental geometrical parameters for the benzoic acid dimer are from x-ray diffraction measurements (Ref. 27).
[c]B3LYP/6-311+G($2d,2p$)/6-31+G(d) (see text).
[d]Assumed in refinement of electron diffraction data.

mal mode. In applying this approach to BAD, all intensity is assumed to derive from the asymmetric OH stretch normal mode, and the dipole is assumed to vary linearly with the stretch coordinate.

The model described above, together with several extensions, was also applied to FAD. First because the CH and OH stretch vibrations have similar frequencies, they are appreciably mixed in the Q_1 and Q_3 normal coordinates, necessitating inclusion of both the CH and OH stretch "bright" states. (The numbering scheme for the normal modes of FAD is given in Table II, below.) Second, because the low frequency interdimer motion R_1 has significant projection onto both the Q_{21} and Q_{23} normal modes, the model was extended to include all states that can be generated by adding up to two quanta in either the Q_{21} and/or Q_{23} modes. In this extended model, intensity can be acquired by mixing with either the OH or the CH stretch vibrations. Third, we investigated using the experimental fundamental frequencies in place of the calculated frequencies as the frequencies of the normal mode basis functions. Finally, FAD is small enough that it was also possible to calculate the vibrational spectrum using the full cubic force field.

IV. ELECTRONIC STRUCTURE RESULTS

For FAD, the geometries were optimized and the harmonic vibrational frequencies were calculated using both the Becke three parameter Lee–Yang–Pair (B3LYP) and second-order Møller–Plesset (MP2) methods. Several basis sets, including 6-31+G(d), 6-311+G($2d,p$), 6-311+G($2d,2p$),[15] aug-cc-pVDZ, and aug-cc-pVTZ,[16] were investigated. A subset of the key geometrical parameters are reported in Table I, and the calculated harmonic frequencies are reported in Table II. For comparative purposes, geometries and frequencies are also reported for the formic acid monomer (FA). It is clear from the results in these Tables that the 6-31+G(d) basis set, which has often been used for such studies in the past, is inadequate for describing the structure and vibrational frequencies of FAD. It is also noteworthy that with the largest basis set considered, the MP2 calculations give shifts in the OH stretch frequencies in going from FA to FAD, about 116 cm^{-1} smaller than those obtained from the B3LYP calculations. Since quadratic CI with single and double excitations (QCISD) calculations (results not tabulated) give harmonic frequencies close to the MP2 values, these results provide strong evidence that the B3LYP method does not provide a quantitatively correct description of this aspect of the H-bonding in the FAD dimer.

For BAD, the B3LYP procedure was used for optimizing the geometry, calculating the harmonic frequencies and normal modes, and for calculating the cubic force field in spite of the concerns raised above, due to the high computational cost of the corresponding MP2-level calculations for molecules of this size. In this case, the geometry was optimized and the harmonic frequencies calculated using two different basis sets, one with a 6-311+G($2d,2p$) description of all atoms and the other a mixed basis set, with a 6-311+G($2d,2p$) description of the atoms of the COOH groups and a 6-31+G(d) description of the C and H atoms associated with the phenyl rings. The key geometrical parameters are nearly identical with these two basis sets, as are the harmonic frequencies, and, for this reason, the smaller basis set was adopted for the calculation of the cubic force field of BAD. Tables I and III report, respectively, the key geometri-

TABLE II. Calculated harmonic and experimental frequencies (cm^{-1}) of formic acid monomer and dimer.

				B3LYP				MP2		
N	Symm.	Coord.[b]	Expt[a]	6-31+G (d)	6-311+G ($2d,p$)	aug-cc-pVDZ	aug-cc-pVTZ	6-311+G ($2d,p$)	aug-c-pVDZ	aug-cc-pVTZ
					Monomer					
1	A'	νOH	3569	3663	3730	3717	3717	3745	3726	3740
2	A'	νCH	2943	3104	3051	3066	3051	3117	3138	3094
3	A'	νC═O	1777	1823	1810	1804	1811	1784	1771	1793
4	A'	δCH	1381	1409	1401	1386	1401	1419	1396	1400
5	A'	δOH	1223	1300	1304	1296	1298	1309	1295	1301
6	A'	νC–O	1105	1137	1122	1124	1122	1120	1116	1130
7	A''	γCH	1033	1047	1050	1046	1051	1052	1047	1056
8	A''	πOH	642	690	677	678	678	674	674	680
9	A'	δCO_2	625	623	630	623	629	632	618	626
					Dimer					
1	B_u	νOH	3110	3245	3173	3154	3161	3255	3255	3305
2	A_g	νCH	2949	3118	3071	3086	3066	3127	3158	3137
3	B_u	νCH	2957	3113	3060	3073	3055	3123	3148	3132
4	A_g	νOH	-	3153	3051	3028	3040	3145	3143	3194
5	B_u	νC═O	1754	1786	1765	1761	1767	1761	1751	1776
6	A_g	νC═O	1670	1722	1691	1687	1693	1696	1688	1711
7	A_g	δOH	1415	1461	1488	1481	1481	1487	1475	1499
8	B_u	δOH	-[c]	1441	1454	1445	1449	1463	1450	1473
9	A_g	δCH	1375	1405	1403	1388	1404	1421	1391	1429
10	B_u	δCH	1362	1398	1402	1387	1402	1414	1386	1422
11	B_u	νC–O	1218	1255	1260	1258	1260	1256	1244	1257
12	A_g	νC–O	1214	1254	1256	1255	1257	1250	1237	1249
13	A_u	γCH	1060	1090	1102	1105	1102	1108	1107	1114
14	B_g	γCH	1050	1070	1077	1078	1079	1082	1079	1085
15	A_u	πOH	917	982	1008	1001	1002	995	980	995
16	B_g	πOH	-	957	988	986	983	975	964	980
17	B_u	δCO_2	699	704	725	717	723	718	702	719
18	A_g	δCO_2	677	687	690	682	690	688	670	688
19	B_u	dimer in-plane rock	248	270	277	284	281	268	274	280
20	B_g	dimer out-of-plane wag	230	257	261	266	262	258	258	269
21	A_g	dimer in-plane rock	190	210	208	214	213	200	209	209
22	A_u	dimer out-of-plane wag	163	181	186	189	187	177	173	183
23	A_g	dimer stretch	137	169	174	178	175	166	169	171
24	A_u	dimer twist	68	78	77	79	78	70	68	69

[a]Reference 28.
[b]Natural internal coordinates are used (Ref. 29) to express symmetry coordinates. For definitions of the coordinates for the formic acid monomer and dimer, see Ref. 30.
[c]Although Ref. 30 assigned a band at 1450 cm^{-1} to this fundamental, we omit it because it does not show up in high-resolution gas-phase spectra (Ref. 31). This assignment was also rejected in Ref. 21.

cal parameters and harmonic frequencies of BAD as well as of the benzoic acid (BA) monomer obtained from the B3LYP/mixed basis set calculations.

The cubic anharmonicity constants of FAD were calculated using the B3LYP and MP2 methods, in both cases, employing the 6-31+G($2d,p$) basis set, whereas those for BAD were calculated using the B3LYP/mixed basis set approach. Table IV summarizes the most important anharmonicity constants from these calculations. For FAD, the B3LYP and MP2 procedures are found to give similar anharmonicity constants, with the MP2 values generally being only about 3%–5% larger than the B3LYP values. This close agreement justifies the use of the B3LYP method for evaluating these constants.

Table V compares for FAD the Fermi resonance coupling terms calculated using the restricted and full force fields. In those cases that the couplings are large in magnitude, the B3LYP and MP2 coupling terms agree to within 30%. The agreement between the coupling constants calculated using the truncated and full cubic force fields (both using the B3LYP method) is less satisfactory. However, even so, the coupling constants calculated using the truncated force field agree to within a factor of 2 (and generally much better) with those from the full force field in all cases that the latter are greater than 30 cm^{-1} in magnitude. This agreement suggests that the main source of the Fermi coupling is *via* the f_{345} stretch-bend coupling. Table V also reports the empirical frequencies and couplings used by Maréchal. Given that this was a restricted empirical fit, one cannot expect more than the rough qualitative agreement that is observed.

TABLE III. Calculated harmonic and experimental frequencies (cm^{-1}) of benzoic acid monomer and dimer.

			Monomer						Dimer		
				B3LYP						B3LYP	
N	Mode[a]	Symm	Exp.[b]	6-31G(d,p)[c]	Mixed[d]	*N*	Symm.	Exp.[e]	6-31G(d,p)[c]	Mixed[d]
	COOH modes									
1	νOH	A'	3567	3763	3773	11	A_g	3350 s	3090	3157
						12	B_u		2966	3055
7	ν(C═O)	A''	1752	1819	1780	13	A_g	1693 s	1759	1725
						14	B_u		1705	1681
12	ν(C–O)	A'	1347	1392	1372	29	A_g	1328	1337	1326
						30	B_u		1334	1314
15	δOH	A'	1169	1218	1216	21	A_g	1424 s	1519	1502
						22	B_u		1481	1470
32	πOH	A''	628	607	594	41	A_u	936 s	1014	1023
						48	B_g		967	973
36	δCO_2	A'		384	383	69	A_g	387 vw	425	424
						72	B_u		391	389
37	Rock	A'		216	216	73	A_g		292	287
						74	B_u		265	262
38	Wag	A''		160	160	75	A_u		189	186
						76	B_g		170	171
39	Twisting	A''		71	66	79	A_u		88	71
						80	B_g		73	71
Intermolecular modes										
	H-bond stretch					77	A_g		120	115
	H-bond shearing					78	A_g		107	107
	Tilting					81	B_g		65	62
	Cogwheel					82	B_u		61	60
	Torsion					83	A_u		35	33
	Butterfly					84	A_u		18	21

[a]The characterization of the atomic displacements corresponding to the normal modes of BA/BAD are taken from Ref. 32.
[b]Determined in an Ar matrix by Reva *et al.* (Ref. 33). Band assignments from Ref. 32.
[c]Reference 32.
[d]B3LYP/6-311+G(2d,2p)/6-31+G(d) (see text).
[e]The frequencies reported for the dimer are taken from spectra of BA in KBr pellets by Sanchez de la Blanca *et al.* (Ref. 34). Band assignments are from Ref. 32.

V. COMPARISON WITH EXPERIMENT

A. Benzoic acid dimer isotopomers

Figure 2 presents stick spectra for the fully protonated [d_0-d_0, Fig. 2(a)], ring-deuterated [d_5-d_5, Fig. 2(b)], and ring-deuterated O–H/O–D [d_5-d_6, Fig. 2(c)] BA dimers, computed using the cubic anharmonic constants and, with the exception of the IR active OH stretch vibration, fundamental frequencies obtained using the B3LYP/mixed basis set calculations. The OH stretch fundamental was assigned a frequency of 2950 cm^{-1}.[6,17] The experimental spectra presented directly above the calculated spectra have been reported previously.[6] This earlier study also reported a spectrum calculated using the force field described in Eq. (8) and using B3LYP force constants, but with the 6-31+G* basis set on all atoms.

TABLE IV. *Ab initio* cubic force constants f_{ijk} in $cm^{-1}/Å^3$ for benzoic acid and formic acid dimers for the potential of Eq. (5).

	FAD		BAD
ijk	B3LYP[a]	MP2[a]	B3LYP[b]
345	55 555	55 802	57 707
255	66 746	57 512	60 188
244	59 621	58 489	61 194
133	32 921	27 166	28 546
122	64 316	57 810	59 747

[a]6-311+G(2d,p) basis set.
[b]Mixed 6-311+G(2d,2p)/6-31+G(d) basis set (see text).

The over-all width and major substructure of the observed bands of the three isotopomers of BAD are remarkably well reproduced by the calculated spectra, particularly in the low-frequency region of the spectrum. For all three isotopomers, the high-frequency region above 2950 cm^{-1} is much more congested in the experimental spectrum than in that calculated using the truncated cubic force field. The calculations reveal that most of the combination bands that gain intensity from coupling to the O–H stretch also have contributions from the C═O stretch (in combination with a vibration that contains some O–H bend character). The cubic anharmonic constants used in the present model (Table V) do not include cubic couplings involving the C═O stretch local mode, which might be anticipated to be coupled to the O–H stretch, since the two groups are H-bonded to one another. It is anticipated that refinement of the model to include this coupling would fill in much of the structure missing in the calculated spectrum.

As our earlier study led us to believe, in all three BAD

TABLE V. Cubic coupling constants (cm^{-1}) in dimensionless normal coordinates for the formic acid dimer.

Energy[a]	Coupling[b]	Coupling[c]	Coupling[d]	Energy[e]	|Coupling|[e]	Assignment
2369	−16.80	−16.06	−19.61			$\delta_{C=O}(Ag)\,\delta_{OCO}(Bu)$
2418	−10.59	−10.34	−7.68			$\delta_{C=O}(Bu)\,\delta_{OCO}(Ag)$
2431	15.71	12.74	39.81	2420	70	$\nu_{C-O}(Bu)\,\nu_{C-O}(Ag)$
2576	−22.00	−13.82	−19.20			$\delta_{CH}(Bu)\,\nu_{C-O}(Ag)$
2592	−11.09	−6.54	−2.29			$\delta_{CH}(Ag)\,\nu_{C-O}(Bu)$
2604	−29.86	−30.00	−55.72			$\delta_{OH}(Bu)\,\nu_{C-O}(Ag)$
2664	−38.15	−35.04	−58.59	2630	95	$\delta_{OH}(Ag)\,\nu_{C-O}(Bu)$
2737	15.46	7.09	−15.01			$\delta_{CH}(Ag)\,\delta_{CH}(Bu)$
2797	20.98	15.40	15.59	2810	40	$\delta_{OH}(Bu)\,\delta_{CH}(Ag)$
2809	53.32	38.01	28.22	2765	45	$\delta_{OH}(Ag)\,\delta_{CH}(Bu)$
2869	72.35	82.54	70.94	2850	55	$\delta_{OH}(Ag)\,\delta_{OH}(Bu)$
2887	−13.95	−12.80	−30.91			$\delta_{C=O}(Ag)\,\nu_{C-O}(Bu)$
2955	−6.56	−5.81	−15.14	2930	45	$\delta_{C=O}(Bu)\,\nu_{C-O}(Ag)$
3032	19.54	13.88	20.66	3025	65	$\delta_{C=O}(Ag)\,\delta_{CH}(Bu)$
3092	26.52	30.15	31.06	3085	70	$\delta_{C=O}(Ag)\,\delta_{OH}(Bu)$
3116	4.62	2.98	9.39			$\delta_{C=O}(Bu)\,\delta_{CH}(Ag)$
3188	15.91	15.98	16.67	3165	25	$\delta_{C=O}(Bu)\,\delta_{OH}(Ag)$

[a]Transition frequencies calculated using experimental fundamental frequencies of Bertie and Michaelin (Ref. 19) with the exception of the $\delta_{OH}(Bu)$ and $\delta_{OH}(Ag)$ modes whose frequencies were taken to be 1447 and 1422 cm^{-1}, respectively.
[b]Couplings calculated with MP2/6-311+G(2*d*,*p*) using Eq. (8).
[c]Couplings calculated with B3LYP/6-311+G(2*d*,*p*) using Eq. (8).
[d]DFT results for full cubic force field.
[e]Results of Maréchal (Ref. 12).

isotopomers, it is the coupling via f_{345} of the B_u O–H stretch with the B_u symmetry combination bands involving the O–H bend that dominates the spectrum. In fact, the O–H stretch/intermolecular stretch coupling (f_{133}), which has often been invoked to explain the appearance of the O–H stretch spectrum in strongly H-bonded dimers, appears not to be important in the spectra of the carboxylic acid dimers. These results are consistent with the conclusion of Marechal.[12] In a series of test calculations we have found that the magnitude of f_{133} would have to be increased from its calculated value by a factor of 5 or more for the structure from the intermolecular stretch to significantly contribute to the breadth and spectral congestion of the spectrum.

B. Formic acid dimer

Figure 3 compares the experimental cavity ringdown spectrum of Ito and Nakanaga [Fig. 3(a)][3] with the stick spectrum computed using the restricted force field analogous to that used for BAD [Fig. 3(b)]. The cubic force constants used in the model are from B3LYP/6-311+G(2*d*,*p*) calculations as are the frequencies, with the exception of the asymmetric OH stretch frequency which was set to 2950 cm^{-1}, the same value as was chosen for BAD.

The poor agreement of the calculated spectrum with experiment is disappointing, with the simple model predicting a spectrum dominated by just two strong IR transitions, whereas the observed spectrum is far more complicated. This raises the question why the reduced cubic force field model works so much better for BAD than FAD.

One possible explanation for the greater success of the reduced model for BAD than for FAD is the larger number of near resonant states in the former. In particular, in FAD the OH local bend modes involve contributions from only the

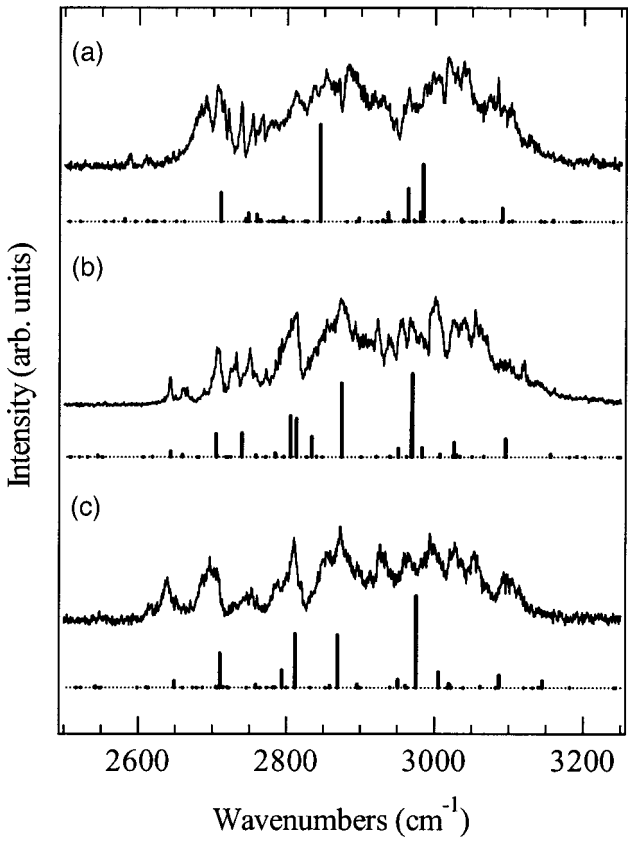

FIG. 2. Calculated stick spectra for the (a) fully protonated (d_0-d_0), (b) ring-deuterated (d_5-d_5), and (c) ring-deuterated/O–H/O–D (d_5-d_6) BA dimers, computed using the cubic anharmonic constants of Table IV. Calculated vibrational frequencies are those from the B3LYP mixed basis set, and have been multiplied by 0.978 to account for the diagonal anharmonicity of the vibrations. The b_u symmetry OH stretch fundamental has been set at 2950 cm^{-1} in all three isotopomers. The experimental spectra are taken from Ref. 6.

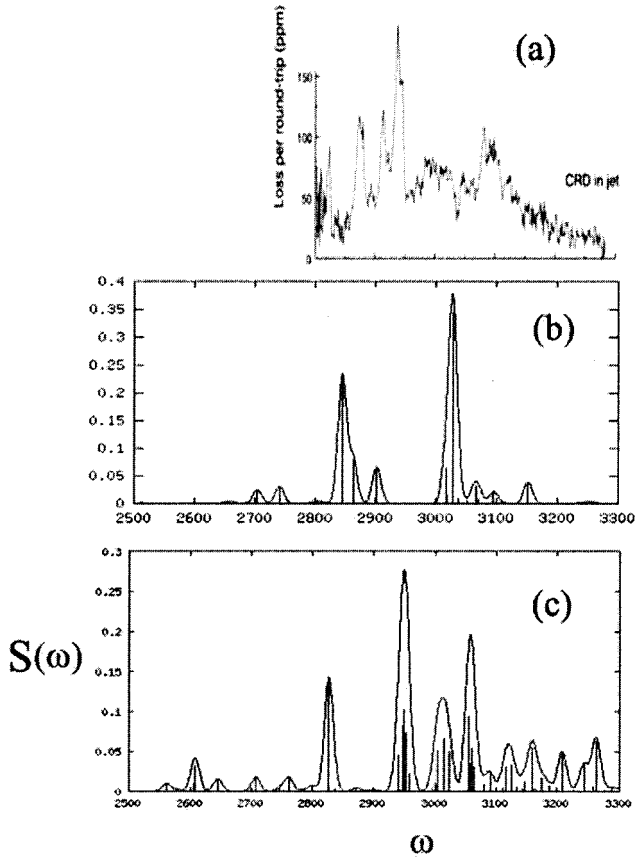

FIG. 3. Comparison of (a) jet-cooled infrared spectrum of the formic acid dimer obtained by Ito and Nakanaga using cavity ring down (CRD) spectroscopy[3] and (b) and (c) $T=0$ K theoretical stick spectra. The spectrum in (b) assumes a restricted cubic force field that couples harmonic modes whose frequencies are obtained using DFT; (c) is calculated using the full cubic force field that couples harmonic oscillators whose frequencies are obtained from experiment and includes contributions from the CH stretch bright state. Also shown are the results of spectral broadening with a Gaussian line shape. See text for details.

OH bend and C═O stretch normal modes, whereas in BAD the CH bends are important as well. The two major peaks in the calculated spectrum of FAD shown in Fig. 3(b) are due to the strong Fermi resonance interaction between the OH bend combination state $\nu_7+\nu_8$ ($1488+1454=2942$ cm^{-1}) and the OH stretch ν_1. The $\nu_5+\nu_7$ ($1765+1488=3253$ cm^{-1}) and $\nu_6+\nu_8$ ($1691+1454=3145$ cm^{-1}) combination states involving OH bends and C═O stretches, are far enough out of resonance to be much less important borrowers of intensity.

For FAD, calculation of the vibrational spectrum using the full *ab initio* or density-functional theory (DFT) cubic force fields is possible. Figure 3(c) shows the stick spectrum of FAD computed using the full B3LYP/6-311+G($2d,p$) cubic force field and experimental values for the fundamental frequencies, with the exception of the A_g OH stretch fundamental which has not yet been observed. The frequency of the A_g OH stretch fundamental was estimated by assuming a splitting of 110 cm^{-1}, close to that obtained in the MP2 calculations, between the two OH stretch fundamentals. This places the A_g OH stretch fundamental at 3000 cm^{-1}. The calculated spectrum is relatively insensitive to this value. As an aside, it should be noted that this motion corresponds to double proton transfer, which our potential model does not describe even qualitatively. The work of Vener *et al.*[18] suggests that one quantum of excitation of this mode is sufficient to surmount the barrier to tunneling.

The intense peak observed at 2937.7 cm^{-1} in the IR spectrum of FAD is due to the CH stretch as has been clearly demonstrated by the isotopic substitution study of Ito and Nakanaga.[3] To obtain a theoretical peak of similar intensity in the calculated spectrum displayed in Fig. 3(c) it was necessary to increase the B3LYP dipole moment derivative for the CH stretch by a factor of 1.4. The surprisingly large intensity of this peak is due to the fact that the CH and OH stretch normal modes are admixtures of the CH and OH stretch local modes; hence the CH stretch vibration borrows its intensity from the OH stretch. Thus, it appears that the B3LYP calculations underestimate the extent of mixing of the OH and CH stretches. With the adjustment of the CH dipole moment derivative, the theoretical spectrum calculated using the full cubic force field and experimental fundamentals is in qualitative agreement with experiment, especially in regard to the broad spectral width and the major contributions to the sub-structure.

Given the striking dissimilarity between the spectra reported in Figs. 3(b) and 3(c), obtained using the truncated and full cubic force fields, respectively, it is worthwhile examining in detail the differences between the two calculations. Figure 4 presents a series of calculated spectra that test the full cubic results against the restricted analysis, with various terms selectively removed or adjusted. Figures 4(a) and 4(b) examine the sensitivity of the calculated spectrum to the choice of the fundamental frequencies for the OH bend vibrations. This test was carried out because there is an ambiguity in the experimental value of the frequency of the B_u OH bend vibration. Although Bertie and Michaelian[19,20] attributed a very weak feature observed near 1450 cm^{-1} to the B_u OH bend vibration, this is in disagreement with force field and electronic structure calculations that place the frequency of the B_u OH bend about 25 cm^{-1} below that of the A_g OH bend vibration. This has led Qian and Krimm to reject the assignment of the weak 1450 cm^{-1} feature to the B_u OH bend vibration.[21] On the other hand, there appears to be a consensus that the fundamental frequency of the symmetric (A_g) OH bend vibration is 1415 cm^{-1}.[19]

The theoretical spectrum reported in Fig. 4(a) was obtained with the choice of 1447 and 1422 cm^{-1} for the frequencies of the A_g and B_u OH bend fundamentals, respectively, with this state ordering and splitting being chosen to be consistent with the MP2 calculations. While this choice places the A_g vibration 32 cm^{-1} higher than experiment, this may simply be a reflection of the need to include higher frequency fundamentals and higher-order couplings. For comparison, Fig. 4(b) retains the Bertie and Michaelian assignments of 1415 and 1450 cm^{-1} for the A_g and B_u OH bends. As such, this figure is the same as Fig. 4(c) with the exception that here we have used the *ab initio* dipole derivatives, with the result that the line corresponding to the CH stretch is less intense. The reversal in ordering of the A_g and B_u bend modes (compared to the Bertie and Michaelian as-

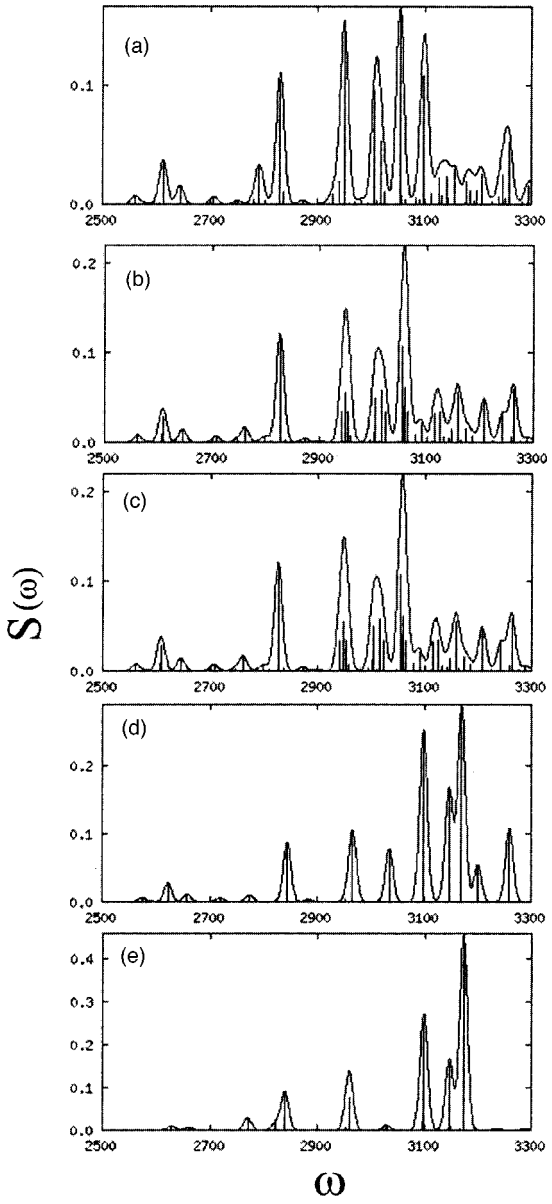

FIG. 4. Comparison of $T=0$ K theoretical FAD stick spectra. Also shown are results of spectral broadening with a Gaussian line shape. (a) model results use full cubic coupling of normal modes with frequencies taken to be experimental fundamental frequencies. All intensities are calculated using DFT values for linear dipoles. The important exceptions are the OH bend frequencies which are chosen to be 1422 and 1447 cm^{-1} for the B_u and A_g modes, respectively. (b) same as (a) but frequencies of bend modes are chosen to be 1450 and 1415 cm^{-1} for the B_u and A_g modes, respectively. (c) same as (b) but calculation does not include coupling terms of the form $Q_i^2 Q_j$ where j corresponds to the low-frequency modes 21 or 23 and $i=1$ or 3, this corresponding to either the OH or CH stretch. Frequency (d) same as (c) but all cubic terms involving the low-frequency modes 21 or 23 are set to zero. (e) same as (b) but the restricted cubic force field is employed. See text for details.

signment) has its most dramatic effect on the relative intensities of the bands, and leads to somewhat better agreement with experiment [Fig. 4(a)].

Figure 4(c) shows the effects of removing the cubic anharmonic terms that couple the OH and CH stretch vibrations ($j=1$ and 4) with the intermolecular stretching modes ($i=21$ and 23) *via* $Q_i Q_j^2$ terms in the potential. As for BAD, the removal of the anharmonic terms produces a second-order effect on the spectrum in which the overall width is retained, but the splittings of several bands on the high-frequency end of the spectrum are lost. In Fig. 4(d), all coupling terms involving the intermolecular stretching modes Q_{21} and Q_{23} have been removed from the spectrum. Again, the overall width of the spectrum is retained. Table VI indicates which combination states are involved in the spectrum reported in Fig. 4(d) and how they contribute to the intensity sharing. These results thereby confirm the dominant role of the stretch-bend coupling term in determining the width of the spectrum of FAD, as it was for that of BAD.

TABLE VI. Transition energies and intensities for FAD results of Fig. 4(d). Each state is labeled with the leading term in the normal mode basis set.

Energy (cm^{-1})	Intensity	|Overlap|[a]	State
2622.5	0.03	0.96	$7_1\,11_1$
2658.2	0.01	0.97	$8_1\,12_1$
2774.3	0.01	0.99	$7_1\,10_1$
2844.4	0.09	0.93	$7_1\,8_1$
2966.4	0.10	0.87	3_1
3035.2	0.08	0.93	$6_1\,10_1$
3098.8	0.25	0.73	$6_1\,8_1$
3146.9	0.17	0.74	$5_1\,7_1$
3169.7	0.29	0.65	$5_1\,7_1$
3200.6	0.05	0.95	$2_1\,19_1$
3259.6	0.11	0.94	$4_1\,19_1$

[a]Magnitude of the overlap between the eigenstate and the basis state.

Figure 4(e) results from using the restricted cubic force field, which includes the low frequency modes. The spectrum of Fig. 4(e) has an appearance very similar to that of Fig. 4(d) above it. This visual comparison makes clear the major difference between the full and restricted cubic anharmonic analyses of FAD; namely, that the calculations with the restricted cubic force field predict very little coupling with the low-frequency modes of the dimer. In general, we find that the restricted analysis significantly underestimates the couplings to the low frequency modes. This is expected to also be the case for BAD. However, as these couplings only make minor contributions to the overall spectral width of the low-temperature spectra of BAD, this is not a serious shortcoming. A second, smaller difference is that in contrast to Fig. 4 there is no peak at 3259 cm^{-1} in the spectrum reported in Fig. 4(e). The 3259 cm^{-1} peak is due to the combination band $\nu_4+\nu_{19}$ ($3000+248=3248\ cm^{-1}$). Here the symmetric and antisymmetric OH stretches are coupled via an antisymmetric dimer stretching mode. This interaction was not included in the restricted model, since only coupling of the OH stretches to the symmetric dimer stretch modes was considered in Eq. (7). To include coupling to antisymmetric dimer stretches, one would need to extend the restricted model by including terms of the form $R_2 R_3 R_6$, where R_6 is the dimer stretch mode of B_u symmetry. One would also need a more realistic treatment of the very anharmonic OH symmetric stretch such as that of Vener *et al.*[18]

The results shown in Fig. 4 indicate that state-by-state agreement with experiment is beyond the scope of the present theoretical calculations because the spectral details are very sensitive to the energies of the combination bands. Nonetheless the central features of the spectrum, in particu-

lar, its width, and the mechanisms responsible for these features have been elucidated and understood with our models.

C. Comparing FAD and BAD

The most notable similarity between the FAD and BAD spectra is that they are very broad (300–550 cm^{-1}), with the width being due to strong Fermi resonance interactions with background states involving excitation of the OH bends and C═O stretches. The low-frequency modes make only minor contributions to the overall width, but they do contribute to the congestion. An important difference between the spectra of these two dimers is that in BAD many additional resonance interactions are possible in the lower frequency region of the spectrum. This is a consequence of the fact that normal mode OH bend vibrations of BAD have contributions from both the OH and CH bends. This leads to a sharing of intensities over many states, which fills in the lower frequency region of the spectrum for BAD. In FAD, the lower frequency portion of the spectra is relatively sparse. A second important difference is that the OH and CH stretch local modes of FAD mix when forming the normal modes. This greatly enhances the intensity of the CH asymmetric stretch vibration in $(HCOOH)_2$ compared to $(HCOOD)_2^3$. and significantly changes the appearance of the low resolution spectrum.

In either case, the remarkable breadth of the OH stretch absorption in the IR spectra of FAD and BAD can be accounted for by the f_{345} term, which is unusually large in these systems. If we were to freeze all the internal coordinates except those described by the R_1-R_5 coordinates of Eq. (4), then the f_{345} force constant maps onto a single cubic coupling term in the normal-mode approximation. In dimensionless coordinates, this coupling constant has a magnitude of 370 cm^{-1}. This means that two states that were exactly degenerate in the absence of coupling would be split by $\Delta E = 2(370)/\sqrt{8} = 260\ cm^{-1}$.[22] Gelussus and Thiel[23] have compiled CH stretch–bend coupling parameters for a number of halocarbons. These are typically between 40 and 100 cm^{-1}, although they do approach 300 cm^{-1} in $CHBr_3$ and CHI_3. The analogous OH stretch–bend anharmonic term of H_2O is 134 cm^{-1}.[24]

VI. CONCLUSIONS

The present work provides a simple physical picture of the dominant cause for the unusual breadth and sub-structure of the O–H stretch infrared spectrum of carboxylic acid dimers. Cubic anharmonic constants were calculated for FAD and BAD using a set of five key internal coordinates that are closely related to the O–H stretch (B_u and A_g), O–H bend (B_u and A_g), and intermolecular stretch (A_g) vibrational modes. It is found that a single cubic anharmonic coupling term (f_{345}), which couples the O–H stretch with appropriate symmetry combination bands accounts for the overall breadth and the dominant sub-structure of the experimental spectra. This term dominates over the f_{133} term that couples the O–H stretch with the intermolecular stretch. A single cubic anharmonicity (f_{345}) can have such a profound effect largely because the ''pure'' O–H bending coordinate included in the model maps onto several normal modes that are spread over several hundred wave numbers. In other words, the component of the O–H bend in several normal modes takes a single $(1+1)$:1 Fermi resonance with the O–H stretch and spreads it over many levels in the 2600–3100 cm^{-1} region consistent with the 500 cm^{-1} width observed experimentally.

While it is satisfying that a single anharmonic constant can account for much of the observed spectra, it is clear that further refinements to the model involving ''second tier couplings'' would further improve the fit. We have already noted that the high frequency end of the spectrum, which involves C═O stretch/O–H bend combination bands, has too little intensity relative to experiment. This points to the need for inclusion of anharmonic terms involving the C═O stretch, which have not been taken into account in the present model.

The present study also shows that B3LYP density functional calculations, when used with a suitably flexible basis set, are able to account in a qualitatively correct manner for the cubic anharmonic coupling constants. Although there are indications from the calculations on FAD, that the MP2 procedure is somewhat more reliable for describing the interactions between the monomers of carboxylic acid dimers, given the other approximations, namely, the truncation in the vibrational basis set and the truncation of the force field at cubic terms, it seems justifiable to adopt the B3LYP procedure for obtaining the harmonic frequencies and the cubic force constants needed for calculating the vibrational spectrum.

Finally, it will be important to extend this model and its refinements to a wider range of strongly H-bonded homo- and heterodimers. Recent experimental data on the 2-pyridone dimer (with its two N–H···O═C H-bonds)[25] and the mixed 2-pyridone/2-hydroxypyridine dimer (with its one N–H···O═C and one OH···N H-bond)[26] would benefit from a similar analysis. Predictions of the spectra for the DNA base pairs and other very strong single XH···Y H-bonded complexes will also stimulate further experiment and a reassessment of existing spectral data in light of the model.

ACKNOWLEDGMENTS

The authors gratefully acknowledge the support of the National Science Foundation for this work (G.M.F. and T.S.Z. under a 2-year extension to CHE9728636; E.L.S. under CHE0072128; and E.M.M. and K.D.J. under CHE0078528). E.L.S. thanks the Vilas Trust of the University of Wisconsin for partial support of this work.

APPENDIX: COORDINATE TRANSFORMATIONS

The internal coordinates are given in Eq. (4). In addition to these coordinates we introduce the constraint for overall rotation [cf. Eq. (A1)] and center of mass translation [cf. Eqs. (A2) and (A3)].

$$R_R = \sum_{i=1}^{N} m_i (x_i z_i^e - z_i x_i^e), \tag{A1}$$

$$R_{\mathrm{Tx}}=\sum_{i=1}^{N} m_i x_i , \tag{A2}$$

$$R_{\mathrm{Tz}}=\sum_{i=1}^{N} m_i z_i . \tag{A3}$$

For benzoic acid there are $N=30$ atoms. Given that we treat the RCOO groups as rigid bodies that are not allowed to rotate and that we are only allowing in-plane motions, the x and z coordinates of atoms 3 and 4 serve to define the values of all the coordinates of these groups. As a result, the above Eqs. (A1)–(A3) reduce to

$$R_R=\alpha(x_3-x_4)+\beta(x_1-x_2)-\gamma(z_3-z_4)-\delta(z_1-z_2), \tag{A4}$$

$$R_{\mathrm{Tx}}=m_{\mathrm{H}}(x_3+x_4)+m_{\mathrm{M}}(x_1+x_2), \tag{A5}$$

$$R_{\mathrm{Tz}}=m_{\mathrm{H}}(z_3+z_4)+m_{\mathrm{M}}(z_1+z_2). \tag{A6}$$

Here m_{M} is the mass of RCOO and m_{H} is the mass of H. The coefficients are defined in terms of the full numbering scheme as follows:

$$\alpha=m_{\mathrm{H}}z_3^e , \tag{A7}$$

$$\gamma=m_{\mathrm{H}}x_3^e , \tag{A8}$$

$$\beta=\sum_{L} m_i z_i^e , \tag{A9}$$

$$\delta=\sum_{L} m_i x_i^e . \tag{A10}$$

The last two summations are over all the atoms in the left, rigid monomer. Rewriting Eq. (4) and Eqs. (A4)–(A6) in matrix form one obtains

$$\begin{pmatrix} R_1 \\ R_2 \\ R_4 \\ R_{\mathrm{R}} \\ R_5 \\ R_{\mathrm{Ty}} \\ R_3 \\ R_{\mathrm{Tz}} \end{pmatrix} = \begin{pmatrix} 0 & 0 & -1 & 0 & 0 & 0 & 0 & 0 \\ 0 & 0 & -1 & 1 & 0 & 0 & 0 & 0 \\ -1 & 1 & 0 & 0 & 0 & 0 & 0 & 0 \\ \beta & \alpha & -\delta & -\gamma & 0 & 0 & 0 & 0 \\ 0 & 0 & 0 & 0 & -1 & 1 & 0 & 0 \\ 0 & 0 & 0 & 0 & m_{\mathrm{M}} & m_{\mathrm{H}} & 0 & 0 \\ 0 & 0 & 0 & 0 & 0 & 0 & -1 & 1 \\ 0 & 0 & 0 & 0 & 0 & 0 & m_{\mathrm{M}} & m_{\mathrm{H}} \end{pmatrix} \begin{pmatrix} x_1-x_2 \\ x_3-x_4 \\ z_1-z_2 \\ z_3-z_4 \\ x_1+x_2 \\ x_3-x_4 \\ z_1+z_2 \\ z_3+z_4 \end{pmatrix} . \tag{A11}$$

The order of the internal coordinates is chosen so that the transformation matrix **B** is block diagonal. Inverting **B** we find

$$\mathbf{B}^{-1}=\begin{pmatrix} f & \gamma g & -\alpha g & g & 0 & 0 & 0 & 0 \\ f & \gamma g & \beta g & g & 0 & 0 & 0 & 0 \\ -1 & 0 & 0 & 0 & 0 & 0 & 0 & 0 \\ -1 & 1 & 0 & 0 & 0 & 0 & 0 & 0 \\ 0 & 0 & 0 & 0 & -m_{\mathrm{H}}/M & 1/M & 0 & 0 \\ 0 & 0 & 0 & 0 & m_{\mathrm{M}}/M & 1/M & 0 & 0 \\ 0 & 0 & 0 & 0 & 0 & 0 & -m_{\mathrm{H}}/M & 1/M \\ 0 & 0 & 0 & 0 & 0 & 0 & m_{\mathrm{M}}/M & 1/M \end{pmatrix}, \tag{A12}$$

where $M=m_{\mathrm{H}}+m_{\mathrm{M}}$, $g=1/(\alpha+\beta)$, and $f=-(\gamma+\delta)g$.

The $\mathbf{B}^{-1}$ matrix allows us to calculate the internal force constants *ab initio* using finite difference methods, since we can arbitrarily extend any one of the above internal coordinates and calculate the corresponding values of the Cartesian displacement coordinates.

[1] G. C. Pimentel and A. L. McClellan, *The Hydrogen Bond* (Freeman, San Francisco, 1960).
[2] F. Ito and T. Nakanaga, Chem. Phys. Lett. **318**, 571 (2000).
[3] F. Ito and T. Nakanaga, Chem. Phys. **277**, 163 (2002).
[4] M. Halupka and W. Sander, Spectrochim. Acta, Part A **54**, 495 (1998).
[5] T. Haber, U. Schmitt, C. Emmeluth, and M. A. Suhm, Faraday Discuss. **118**, 331 (2001).
[6] G. M. Florio, E. L. Silbert III, and T. S. Zwier, Faraday Discuss. **118**, (Cluster Dynamics), 315 (2001).
[7] S. Bratos and D. Hadzi, J. Chem. Phys. **27**, 991 (1957).
[8] N. Sheppard, in *Hydrogen Bonding*, edited by D. Hadzi (Pergamon, London, 1959), p. 85.
[9] D. Chamma and O. Henri-Rousseau, Chem. Phys. **248**, 53 (1999).
[10] Y. Marechal and A. Witkowski, J. Chem. Phys. **48**, 3697 (1968).
[11] M. J. Wojcik, A. Y. Hirakwawa, and M. Tsuboi, Int. J. Quantum Chem., Quantum Biol. Symp. **13**, 133 (1986).
[12] Y. Marechal, J. Chem. Phys. **87**, 6344 (1987).
[13] Y. Marechal, Chem. Phys. **79**, 69 (1983); **79**, 85 (1983).
[14] E. B. Wilson, J. C. Decius, and P. C. Cross, *Molecular Vibrations* (Dover, New York, 1955).
[15] T. Clark, J. Chandrasekhar, G. W. Spitznagel, and P. v. R. Schleyer, J. Comput. Chem. **4**, 294 (1983); M. J. Frisch, J. A. Pople, and J. S. Binkley, J. Chem. Phys. **80**, 3265 (1984).
[16] R. H. Kendall, T. H. Dunning, Jr. and R. J. Harrison, J. Chem. Phys. **96**, 6796 (1992); D. E. Woon and T. H. Dunning, Jr., *ibid.* **98**, 1358 (1993).
[17] The harmonic frequencies for the $h5$-$h5$ and $d5$-$d6$ dimers are 3150 and 3100 cm^{-1}, respectively. The choice of 2950 cm^{-1} for the OH stretch fundamental corrects for the large anharmonicity anticipated for this vi-

bration, and places the fundamental in its approximately correct position by comparison with experiment.
[18] M. V. Vener, O. Kühn, and J. M. Bowman, Chem. Phys. Lett. **349**, 562 (2001).
[19] J. E. Bertie and K. H. Michaelian, J. Chem. Phys. **76**, 886 (1982).
[20] J. E. Bertie, K. H. Michaelian, H. H. Eysel, and D. Hager, J. Chem. Phys. **85**, 4779 (1986).
[21] W. Qian and S. Krimm, J. Phys. Chem. A **102**, 659 (1998).
[22] The factor of $\sqrt{8}$ comes from the raising and lowering operators each carrying a $\sqrt{2}$ in the denominator.
[23] A. Gelessus and W. Thiel, Ber. Bunsenges. Phys. Chem. **99**, 514 (1995).
[24] L. Halonen and J. Tucker Carrington, J. Chem. Phys. **88**, 4171 (1988).
[25] Y. Matsuda, T. Ebata, and N. Mikami, J. Chem. Phys. **110**, 8397 (1999).
[26] D. R. Borst, G. M. Florio, A. Muller, D. W. Pratt, T. S. Zwier, and S. Leutwyler, Chem. Phys. **238**, 341 (2002).
[27] G. Bruno and L. Randaccio, Acta Crystallogr., Sect. B: Struct. Crystallogr. Cryst. Chem. **36**, 1711 (1980); **36**, 2857 (1980).
[28] A. Almenningen, O. Bastiansen, and T. Motzfeld, Acta Chem. Scand. **23**, 2848 (1969); **24**, 747 (1970); M. D. Harmony *et al.*, J. Phys. Chem. Ref. Data **8**, 619 (1979).
[29] G. Fogarasi, X. Zhou, P. W. Taylor, and P. Pulay, J. Am. Chem. Soc. **114**, 8191 (1992).
[30] I. Wolfs and H. O. Desseyn, J. Mol. Struct.: THEOCHEM **360**, 81 (1996).
[31] T. Wachs, D. Borchardt, and S. H. Bauer, Spectrochim. Acta, Part A **43**, 965 (1987).
[32] M. A. Palafox, J. L. Nunez, and M. Gil, Int. J. Quantum Chem. **89**, 1 (2002).
[33] S. G. Stepanian, I. D. Reva, E. D. Radchenko, and G. G. Sheina, Vib. Spectrosc. **11**, 123 (1996); **107**, 3902 (1996).
[34] E. S. de la Blanca, J. L. Nunez, and P. Martinez, An. Quim. Ser. A **82**, 480 (1986).